CONTENTS

1

Sensorless speed control of PMSM

D. Shah*, G. Espinosa–Pérez**, R. Ortega* and M. Hilairet***

* *Laboratoire des Signaux et Systèmes, CNRS–SUPELEC, 91192 Gif–sur–Yvette, France. E-mail:ortega{shah}@lss.supelec.fr*
** *Facultad de Ingeniería–UNAM, Edificio Posgrado 2do. piso, Ciudad Universitaria, 04510 México D.F., MEXICO. E-mail: gerardoe@unam.mx*
*** *Laboratoire de Genie Electrique de Paris, CNRS–SUPELEC, 91192 Gif–sur–Yvette, France. E-mail: hilairet@lgep.supelec.fr*

1.1 Introduction

Sensorless control of electrical machines is a topic that imposes the challenging problem of eliminating the use of sensors for mechanical variables (position and speed) for controller design purposes (Rajashekara *et al.* 1996). Its solution is both important from the applications perspective (due to its economic impact) and quite attractive from the control theory approach (for the mathematical complexity that it exhibits). In spite of the maturity level achieved for understanding the usual strategies implemented in industrial applications as well as in the proposition of novel control schemes (Dawson *et al.* 1998; Khorrami *et al.* 2003; Nam 2010; Ortega *et al.* 1998), the sensorless control problem is currently recognized as a longstanding essentially open problem.

In this paper we are interested in the sensorless control for non–salient permanent magnet synchronous motors (PMSM). For solving it, three variables must be estimated out of the measurement of the electrical coordinates: rotor position and speed, and load torque—the latter assumed constant. Heuristically conceived solutions for this problem abound in the literature, see *e.g.* (Fabio *et al.* 2010; Ichikawa *et al.* 2006) for recent surveys. Many results are also available for the (practically unrealistic) cases of known initial position (Ezzat *et al.* 2010; Tomei and Verrelli 2008) or zero load torque (Ezzat *et al.* 2010a), or the (theoretically unjustifiable) assumption of bounded trajectories (Ezzat *et al.* 2010). An approximate stability analysis of the scheme proposed in (Matsui 1996) is carried out in (Nahid *et al.* 2001). In (Marino *et al.* 2008) a probably stable sensorless scheme for wound rotor synchronous motors is proposed. A key difference of the latter machine with the PMSM

is the availability of flux measurements that considerably simplifies the observation problem. The observability properties of PMSMs have been recently studied in (Ezzat *et al.* 2010a; Ortega *et al.* 2011; Zaltni *et al.* 2009).

Among other techniques, like the use of high frequency electric variables or the implementation of extended Kalman filters, for non–salient pole PMSMs (also known as "surface mounted" PMSMs) the simplest and most common rotor position estimation strategy considers the estimation of the back–emf induced by the permanent magnets (Ichikawa *et al.* 2006), hence it is adopted in this paper. However, instead of using standard methods, that are difficult to tune for standstill and low–speed regimes, it is considered the globally (under some conditions, even exponentially) stable position observer reported in (Ortega *et al.* 2011), which has been successfully evaluated in an experimental setting, combining it with an *ad–hoc* linear speed estimator and a standard field–oriented controller (Lee *et al.* 2010), but without a theoretical justification.

The main objective of this paper is to prove that direct application of two well–established design methodologies—immersion and invariance (I&I) (Astolfi *et al.* 2007) for the observer, and interconnection and damping assignment passivity–based control (IDA–PBC) (Ortega and Garcia–Canseco 2004) for the control—can be combined with the observer of (Ortega *et al.* 2011) to design an asymptotically stable sensorless controller. The result builds upon some preliminary work reported in (Ortega *et al.* 2011; Shah *et al.* 2009) where, assuming *position is known*, I&I techniques are used to design a speed and load torque observer, and in (Akrad *et al.* 2007; Petrovic *et al.* 2001) where *full state–feedback*, globally convergent, IDA–PBCs for the PMSM are proposed. To the best of our knowledge, this is the first time a complete theoretical analysis of a sensorless controller is done—under reasonable practical and theoretical assumptions.

The remaining of the paper is organized as follows. The models of the PMSM and the problem formulation are given in Section 1.2. The controller structure and the main result are presented in Section 1.3. In Section 1.4 the limitations of a linearization–based design are highlighted. A full information IDA–PBC is given in Section 1.5. Section 1.6 recalls the position observer of (Ortega *et al.* 2011), while in Section 1.7 a new I&I speed and load torque observer is proposed. The proof of the main result is given in Section 1.8. Some simulation and experimental results are given in Section 1.9, including a comparison with the heuristic controller of (Lee *et al.* 2010). Finally, we wrap–up the paper with concluding remarks in Section 1.10.

1.2 PMSM models and problem formulation

The classical fixed–frame ($\alpha\beta$) model of the unsaturated non–salient PMSM is given by (Chiasson 2005; Krause 1986)

$$\begin{aligned} L\frac{di_{\alpha\beta}}{dt} &= -Ri_{\alpha\beta} - n_p\omega\Phi\mathcal{J}\left[\begin{array}{c}\cos(\theta)\\ \sin(\theta)\end{array}\right] + v_{\alpha\beta}\\ J\dot{\omega} &= n_p\Phi i_{\alpha\beta}^{\top}\mathcal{J}\left[\begin{array}{c}\cos(\theta)\\ \sin(\theta)\end{array}\right] - \tau_L\\ \dot{\theta} &= n_p\omega \end{aligned} \tag{1.1}$$

where $\mathcal{J} := \begin{bmatrix} 0 & -1 \\ 1 & 0 \end{bmatrix}$, $i_{\alpha\beta} = \begin{bmatrix} i_\alpha \\ i_\beta \end{bmatrix}$ and $v_{\alpha\beta} = \begin{bmatrix} v_\alpha \\ v_\beta \end{bmatrix}$ are the stator currents and motor terminal voltages, respectively, ω is the rotor angular velocity, with $\frac{1}{n_p}\theta$ the corresponding position, L is the stator inductance, R is the stator resistance, n_p is the number of pole pairs, J is the moment of inertia (normalized with n_p), Φ is the magnetic flux and τ_L is the load torque, which is assumed *constant*, but unknown.

To design the observer it is convenient to embed the dynamics (1.1) into the higher–dimensional system

$$L\frac{di_{\alpha\beta}}{dt} = -Ri_{\alpha\beta} - n_p\omega\Phi\mathcal{J}\rho_{\alpha\beta} + v_{\alpha\beta} \tag{1.2}$$

$$J\dot{\omega} = n_p\Phi i_{\alpha\beta}^\top\mathcal{J}\rho_{\alpha\beta} - \tau_L \tag{1.3}$$

$$\dot{\rho}_{\alpha\beta} = n_p\omega\mathcal{J}\rho_{\alpha\beta} \tag{1.4}$$

where the vector

$$\rho_{\alpha\beta} := \begin{bmatrix} \rho_\alpha \\ \rho_\beta \end{bmatrix} = \begin{bmatrix} \cos(\theta) \\ \sin(\theta) \end{bmatrix}, \tag{1.5}$$

is defined. Notice that, if $\rho_{\alpha\beta}$ is known, θ can be easily reconstructed inverting the trigonometric functions.

The model (1.1) can be written in rotating (dq) coordinates by means of the transformation

$$e^{\mathcal{J}\theta} = \begin{bmatrix} \cos(\theta) & -\sin(\theta) \\ \sin(\theta) & \cos(\theta) \end{bmatrix} = \rho_\alpha I_2 + \rho_\beta\mathcal{J}, \tag{1.6}$$

with I_2 the 2×2 identity matrix, to obtain

$$\begin{aligned} L\frac{di}{dt} &= -(RI_2 + n_p\omega L\mathcal{J})i - n_p\omega\Phi\mathcal{J}e_1 + v \\ J\dot{\omega} &= n_p\Phi i_2 - \tau_L \\ \dot{\theta} &= n_p\omega, \end{aligned} \tag{1.7}$$

where the rotated signals

$$i = \begin{bmatrix} i_1 \\ i_2 \end{bmatrix} := e^{-\mathcal{J}\theta}i_{\alpha\beta},\ v = \begin{bmatrix} v_1 \\ v_2 \end{bmatrix} := e^{-\mathcal{J}\theta}v_{\alpha\beta},\ e_1 = \begin{bmatrix} 1 \\ 0 \end{bmatrix} := e^{-\mathcal{J}\theta}\rho_{\alpha\beta}, \tag{1.8}$$

are defined.

Remark 1. The main advantage of the dq–model is that it transforms the periodic orbits associated to the constant speed operation of the $\alpha\beta$ model of the PMSM into equilibrium points. See Subsection 1.5.2.

Remark 2. The industry standard field–oriented control (Nam 2010) is designed for this model, hence the need to reconstruct θ. Indeed, it must be recalled that the input is $v_{\alpha\beta}$ while the measurable output is $i_{\alpha\beta}$, but θ is an *unmeasurable* variable.

1.2.1 Problem formulation

The main contribution of the paper is the solution of the following.

Sensorless control problem. *Consider the PMSM model (1.2)–(1.4) with some desired constant speed $\omega^\star \neq 0$, under the following conditions.*

A.1 *The only variables available for measurement are* $i_{\alpha\beta}$.

A.2 *The load torque* τ_L *is constant but* unknown.

A.3 *The parameters* R, L, Φ *and* J *are known.*

Design an output–feedback controller that ensures the existence of a set of initial conditions, which guarantees that all signals are bounded and that $\omega(t)$ *converges,* exponentially fast*, to* $\omega^\star$.

Remark 3. Even though we have restricted to the case of constant desired speed and constant load torque, it is clear that the controller, being exponentially stable hence robust, will be able to track (slowly) time–varying references and reject changes in the load torque. Interestingly, the simulations and experimental results of Section 1.9 show that the proposed controller yields a good performance even in the face of fast changes in the speed reference and the load torque. The constraint that $\omega^\star \neq 0$ is necessary in the present (sensorless) context, because it is easy to show, see *e.g.*, (Ezzat *et al.* 2010a; Ortega *et al.* 2011; Zaltni *et al.* 2009), that the rank condition for observability is violated when the motor is at standstill. Practically, this assumption is not restrictive because, once again, the intrinsic robustness of the controller accommodates sign changes in the desired speed.

1.3 Controller structure and main result

To simplify the presentation of the main result it is convenient to explain the controller structure and define the notation. The proposed controller is a fourth–order certainty–equivalent version of a full–information globally asymptotically stabilizing controller, which is a static state–feedback IDA–PBC of the form $v_{\alpha\beta} = q(\rho_{\alpha\beta}, \omega, \tau_L, i_{\alpha\beta})$.

The certainty equivalent version is obtained replacing $\rho_{\alpha\beta}, \omega, \tau_L$ by their estimates. The dynamics of the controller is, then, due to the I&I observer, which generates the estimates that we denote $\hat{\rho}_{\alpha\beta}, \hat{\omega}, \hat{\tau}_L$, respectively. The controller, combined with the third–order PMSM dynamics (1.7) yields a seventh–order closed–loop system.

As usual, the analysis is carried–out in error coordinates, which is a mixture of regulation errors, $(\cdot) - (\cdot)^\star$, and estimation errors, $\widehat{(\cdot)} - (\cdot)$. To simplify the notation, all these errors are lumped into a seventh–dimensional vector denoted χ, and defined as[1]

$$\chi = \begin{bmatrix} \chi_1 \\ \chi_2 \\ \chi_3 \\ \chi_4 \\ \chi_5 \\ \chi_6 \\ \chi_7 \end{bmatrix} := \begin{bmatrix} L(i - i^\star) \\ J(\omega - \omega^\star) \\ e^{-\mathcal{J}\theta}\left(\hat{\rho}_{\alpha\beta} - \rho_{\alpha\beta}\right) \\ \hat{\omega} - \omega \\ \hat{\tau}_L - \tau_L \end{bmatrix}. \tag{1.9}$$

Notice that the errors in both, the currents and the vector $\rho_{\alpha\beta}$, are defined in the dq coordinates.

Our main result is the following proposition, whose proof is given in Subsection 1.8.4.

[1]The constants L and J are introduced because—consistent with the Hamiltonian formulation—the IDA–PBC is derived with the motor dynamics represented using the energy variables, flux and momenta.

Proposition 1.3.1 *There exists a fourth–order observer–based speed regulator of the form*

$$\begin{aligned}\dot{\psi} &= g(\psi, i_{\alpha\beta}, v_{\alpha\beta})\\ \begin{bmatrix} \hat{\rho}_{\alpha\beta} \\ \hat{\omega} \\ \hat{\tau}_L \end{bmatrix} &= h(\psi, i_{\alpha\beta}, v_{\alpha\beta})\\ v_{\alpha\beta} &= q(\hat{\rho}_{\alpha\beta}, \hat{\omega}, \hat{\tau}_L, i_{\alpha\beta})\end{aligned}$$

where $\psi \in \mathbf{R}^4$ and g, h, q are suitably defined functions that solves the sensorless control problem[2]*. More precisely, the closed–loop error dynamics is described by a differential equation of the form*

$$\dot{\chi} = f(\chi), \tag{1.10}$$

with zero a (locally) exponentially stable *equilibrium. Consequently, there exist constants $m, \epsilon, \alpha > 0$ such that the following implication holds*

$$\left(|\chi(0)| \leq \epsilon \;\Rightarrow\; |\chi(t)| \leq me^{-\alpha t}|\chi(0)|\right),$$

for all $t \geq 0$, where $|\cdot|$ is the Euclidean norm.

1.4 Unavailability of a linearization–based design

Before proceeding with the design of a controller for the nonlinear model it is natural to explore the possibility of basing the design on the PMSMs linearization. This question is particularly relevant in our case since, as explained below, the stability analysis of the proposed controller relies on the linearization of the closed–loop.

To answer this question, it is convenient to work with the dq model (1.7), with measurable output signals the currents $i_{\alpha\beta}$. Fixing a constant desired speed $\omega^\star$, and its corresponding constant equilibrium current $i^\star$, define the error signals

$$\delta_x(t) = \begin{bmatrix} i(t) - i^\star \\ \omega(t) - \omega^\star \\ \theta(t) - \theta^\star(t) \end{bmatrix}, \; \delta_v := v - v^\star,$$

where $\theta^\star(t) = \theta(0) + \omega^\star t$, and $v^\star$ is the constant control signal that assigns the equilibrium $(i^\star, \omega^\star)$. Now, as the measurable signal is $i_{\alpha\beta}$, invoking (1.8) we define the "output" error

$$\delta_y(t) := e^{\mathcal{J}\theta(t)} i(t) - e^{\mathcal{J}\theta^\star(t)} i^\star.$$

The linearization of (1.7) and the output map above, along the equilibrium trajectory, yields the linear time–varying system

$$\begin{aligned}\dot{\delta}_x &= A_\ell \delta_x + B\delta_v\\ \delta_y &= C(t)\delta_x,\end{aligned}$$

[2]The output–feedback controller consists of (1.18), the position observer (1.23), (1.25) and the speed–load torque observer (1.30).

where

$$A_\ell := \begin{bmatrix} -(\frac{R}{L} I_2 + n_p \omega^\star \mathcal{J}) & -n_p \mathcal{J}(\frac{\Phi}{L} e_1 + i^\star) & 0 \\ \frac{n_p}{J} \Phi e_1^\top \mathcal{J}^\top & 0 & 0 \\ 0 & n_p & 0 \end{bmatrix}, \; B := \begin{bmatrix} \frac{1}{L} I_2 \\ 0 \\ 0 \end{bmatrix}$$

$$C(t) := \begin{bmatrix} e^{\mathcal{J}\theta^\star(t)} & 0 & e^{\mathcal{J}\theta^\star(t)} \mathcal{J} i^\star \end{bmatrix}.$$

Although, apparently, this is an innocuous linear time–varying system for which an observer–based controller could be designed, there are several aspects that stymies this task. First of all, the *equilibrium is unknown* because, on one hand, $i^\star$ depends on the unknown load torque τ_L. On the other hand, the position $\theta^\star(t)$ is also unknown, due to its dependence on $\theta(0)$—see the remark below. Consequently, the system coefficients are unknown. On top of that, the "output" δ_y is known up to the bias term $e^{\mathcal{J}\theta^\star(t)} i^\star$. In summary, since there exist products of unknown parameters and the unmeasurable state ω, designing an output–feedback controller implies the solution of a nonlinearly parameterized adaptive observer problem that—to the best of our knowledge—is not possible with existing techniques.

Remark 4. It is sometimes argued that the motor operation often starts at a known rotor position, hence $\theta^\star(t)$ can be computed. It is obvious that this "trajectory–dependent" controller suffers, in the face of disturbances, from serious robustness problems—that, as is well–known, is the main drawback of schemes based on open–loop integration.

1.5 Full information control

In this section a full–information IDA–PBC, *e.g.*, assuming known the state and the load torque, similar to the one reported in (Akrad *et al.* 2007; Petrovic *et al.* 2001), is presented. This scheme serves as a basis for our certainty–equivalent design.

1.5.1 Port–Hamiltonian model

Following the IDA–PBC methodology (Ortega *et al.* 2002; Ortega and Garcia–Canseco 2004) it is convenient to write the system dynamics in port–Hamiltonian form (van der Schaft 2000), thus we define the state vector as

$$x = \begin{bmatrix} x_{12} \\ x_3 \end{bmatrix} = \begin{bmatrix} Li \\ J\omega \end{bmatrix} \tag{1.11}$$

and the energy function $H(x) = \frac{1}{2} x^\top Q x$, with

$$Q = \begin{bmatrix} \frac{1}{L} I_2 & 0 \\ 0 & \frac{1}{J} \end{bmatrix}. \tag{1.12}$$

Then, the dq system (1.7) can be written in the form

$$\dot{x} = F(x) \nabla H(x) + \begin{bmatrix} v \\ -\tau_L \end{bmatrix} \tag{1.13}$$

where $\nabla = (\frac{\partial}{\partial x})^\top$ and the interconnection and damping matrices are lumped into

$$F(x) = \begin{bmatrix} -R I_2 & -n_p \mathcal{J}(x_{12} + \Phi e_1) \\ n_p (x_{12} + \Phi e_1)^\top \mathcal{J}^\top & 0 \end{bmatrix}.$$

Notice that $\dot{H} = -R|i|^2 + v^\top i - \tau_L \omega$, which is the power balance equation for the motor.

The assignable equilibrium set for (1.13) is given by

$$\{x^\star \in \mathbf{R}^3 \mid x_2^\star = \frac{L}{n_p \Phi} \tau_L\},$$

with $x_1^\star$ and $x_3^\star$ arbitrary. Consistent with engineering practice, and without loss of generality, we will fix $x_1^\star = 0$ in the sequel. See the remark below.

The objective of IDA–PBC is to find a state–feedback control law $v = v(x)$ that assigns to the closed–loop a desired energy function, say $H_d(x)$, which satisfies $x^\star = \arg\min H_d(x)$. This is achieved modifying the interconnection and damping matrices, endowing the closed–loop with the port–Hamiltonian form

$$\dot{x} = F_d(x) \nabla H_d(x), \tag{1.14}$$

where $F_d(x) + F_d^\top(x) \leq 0$. This ensures stability of the equilibrium $x^\star$ with Lyapunov function $H_d(x)$. Under some standard detectability assumptions, *e.g.*, Lemma 3.8 of (van der Schaft 2000), the equilibrium is shown to be asymptotically stable.

1.5.2 A full–information IDA–PBC

Proposition 1.5.1 *Consider the PMSM dq model (1.13) with a desired equilibrium point*

$$x^\star = \begin{bmatrix} 0 \\ \frac{L}{n_p \Phi} \tau_L \\ J\omega^\star \end{bmatrix}. \tag{1.15}$$

The full–information control

$$v^{FI} = d x_{12} + \begin{bmatrix} -\frac{L}{J\Phi} \tau_L x_3 \\ n_p \Phi \omega^\star + \frac{r}{n_p \Phi} \tau_L \end{bmatrix}, \tag{1.16}$$

where $d := \frac{R-r}{L}$, with $r > 0$ a damping injection term, renders $x^\star$ globally asymptotically stable.

Proof. Define the desired closed–loop energy function as the quadratic in the errors form

$$H_d(\chi_{13}) = \frac{1}{2} \chi_{13}^\top Q \chi_{13},$$

with

$$\chi_{13} = \begin{bmatrix} \chi_{12} \\ \chi_3 \end{bmatrix} = \begin{bmatrix} x_{12} - x_{12}^\star \\ x_3 - x_3^\star \end{bmatrix},$$

where Q is as in (1.12).

In order to achieve the required matching between the right hand sides of (1.13) and (1.14), it is considered that matrix $F_d(x)$ is partitioned in an appropriate way, with elements given by $F_{ij}(x)$, that $x_1^\star = 0$ and the definition of $x_2^\star$ in (1.15). Thus, the third row of this marching equation, which actually states the only constraint to be solved since the first and second

components can be easily satisfied with a suitable selection of the control inputs v_1 and v_2, can be written in an equivalent way as

$$\frac{n_p\Phi}{L}\chi_2 = \frac{1}{L}F_{31}\chi_1 + \frac{1}{L}F_{32}\chi_2 + \frac{1}{J}F_{33}\chi_3.$$

Then it is immediate to recognize that a solution is given by

$$F_{31} = F_{33} = 0; \;\; F_{32} = n_p\Phi.$$

The non–positivity condition on the symmetric part of $F_d(x)$ suggests to define $F_{23} = -F_{32} = -n_p\Phi$. Replacing this choice in the second row of the matching equation yields

$$-\frac{R}{L}x_2 - \frac{n_p}{J}x_1x_3 + v_2 = \frac{1}{L}F_{21}x_1 + \frac{1}{L}F_{22}(x_2 - x_2^\star) + \frac{n_p\Phi}{J}x_3^\star,$$

where the term $\frac{n_p}{J}\Phi x_3$ has been canceled. A solution to this equation is obtained selecting $F_{21} = -\frac{Ln_p}{J}x_3$, $F_{22} = -r$ and

$$v_2 = dx_2 + \frac{r}{L}x_2^\star + \frac{n_p\Phi}{J}x_3^\star,$$

which, upon replacement of the definitions of $x_2^\star$ and $x_3^\star$, yields the expression given in the proposition. With the definitions given up to this point, the third component of the matching equation can be satisfied taking $F_{11} = -r$, $F_{12} = \frac{Ln_p}{J}x_3$, $F_{13} = 0$ and

$$v_1 = dx_1 - \frac{n_p}{J}x_2^\star x_3$$

Finally, the closed–loop system takes the desired port–Hamiltonian form (1.14) with

$$F_d(x) = \begin{bmatrix} -r & \frac{Ln_p}{J}x_3 & 0 \\ -\frac{Ln_p}{J}x_3 & -r & -n_p\Phi \\ 0 & n_p\Phi & 0 \end{bmatrix}, \tag{1.17}$$

hence the equilibrium $x^\star$ is stable. Asymptotic stability follows verifying that

$$\dot{H}_d = -\frac{r}{L^2}|\chi_{12}|^2$$

and that $|\chi_{12}|^2$ is a detectable output for the closed–loop system (1.14). $\nabla\nabla\nabla$

1.5.3 Certainty–equivalent sensorless controller

If the states are measurable, the control law to be practically implemented is obtained combining (1.16) with

$$v_{\alpha\beta}^{FI} = e^{\mathcal{J}\theta}v^{FI} = (\rho_\alpha I_2 + \rho_\beta\mathcal{J})v^{FI}.$$

However, under the impossibility for measuring the states $\rho_{\alpha\beta}$, ω and the unknown nature of the perturbation τ_L the proposed *implementable* sensorless controller takes the form

$$\begin{aligned} v_{\alpha\beta} &= (\hat{\rho}_\alpha I_2 + \hat{\rho}_\beta\mathcal{J})\hat{v} \\ \hat{v} &:= dx_{12} + \begin{bmatrix} -\frac{L}{\Phi}\hat{\tau}_L\hat{\omega} \\ n_p\Phi\omega^\star + \frac{r}{n_p\Phi}\hat{\tau}_L \end{bmatrix}. \end{aligned} \tag{1.18}$$

Notice that since the controller in dq coordinates requires the currents x_{12} then its implementable structure is given in terms of the estimated currents in the $\alpha\beta$ reference frame given by $(\hat{\rho}_\alpha I_2 + \hat{\rho}_\beta \mathcal{J})x_{12}$.

1.6 Position observer of (Ortega *et al.* 2011)

In this section the observer presented in (Ortega *et al.* 2011), which estimates the rotor position θ via the observation of the flux, is briefly revisited. Also, an alternative representation of the observer, which is instrumental for the speed–load torque observer given in the next section, is presented. Before presenting the results a word on notation is in order. To facilitate the reference to (Ortega *et al.* 2011), the notation used in this paper is kept here. In particular, we define the observation error $\tilde{\lambda} := \hat{\lambda} - \lambda$, with λ the stator flux and $\hat{\lambda}$ its estimate.

1.6.1 Flux observer and stability properties

In PMSMs the stator flux, λ, is related with the currents and voltages via (Krause 1986)

$$\lambda = Li_{\alpha\beta} + \Phi\rho_{\alpha\beta}. \tag{1.19}$$

Therefore, (1.2) can be equivalently written as

$$\dot{\lambda} = -Ri_{\alpha\beta} + v_{\alpha\beta}. \tag{1.20}$$

This representation of the electrical dynamics of the PMSM is used in (Ortega *et al.* 2011) to develop a position observer. To explain this observer, we make the important observations that $\dot{\lambda}$ is measurable, and that the vector function

$$\eta(\lambda) := \lambda - Li_{\alpha\beta}, \tag{1.21}$$

satisfies

$$|\eta(\lambda)| = \Phi. \tag{1.22}$$

In (Ortega *et al.* 2011) it is shown that

$$\dot{\hat{\lambda}} = -Ri_{\alpha\beta} + v_{\alpha\beta} + \gamma\eta(\hat{\lambda})[\Phi^2 - |\eta(\hat{\lambda})|^2], \tag{1.23}$$

where $\gamma > 0$ is an observer gain, is a gradient descent observer for the flux. It is also proven that the dynamics of the observation error $\tilde{\lambda}$ is described by the second order non–autonomous equation

$$\dot{\tilde{\lambda}} = -\gamma[|\tilde{\lambda}|^2 + 2\Phi\tilde{\lambda}^\top\rho_{\alpha\beta}(t)][\tilde{\lambda} + \Phi\rho_{\alpha\beta}(t)], \tag{1.24}$$

which enjoys the following remarkable stability properties.

P1. *(Global stability)* For arbitrary speeds, the disk

$$\{\tilde{\lambda} \in \mathbf{R}^2 | \, |\tilde{\lambda}| \leq 2\Phi\},$$

is globally attractive. This means, that all trajectories of (1.24) will converge to this disk.

P2. *(Exponential stability under persistent excitation)* The zero equilibrium of (1.24) is exponentially stable if there exists constants $T, \Delta > 0$ such that

$$\frac{1}{T}\int_t^{t+T} \omega^2(s)ds \geq \Delta,$$

for all $t \geq 0$.

P3. *(Constant non–zero speed)* If the speed is constant and satisfies

$$|\omega| > \frac{1}{4}\gamma\Phi^2,$$

then the origin is the unique equilibrium of (1.24) and it is globally asymptotically stable[3].

1.6.2 Description of the observer in terms of $\rho_{\alpha\beta}$

Instrumental for the development of the position and load–torque observer, as well as for the analysis of the closed–loop system, is the representation of the previous flux observer, and its estimation error, in terms of $\rho_{\alpha\beta}$.

Proposition 1.6.1 *From (1.19) and the observer (1.23) define the estimate*

$$\hat{\rho}_{\alpha\beta} = \frac{1}{\Phi}\left(\hat{\lambda} - Li_{\alpha\beta}\right) \tag{1.25}$$

and the error $\tilde{\rho}_{\alpha\beta} := \hat{\rho}_{\alpha\beta} - \rho_{\alpha\beta}$. The observer (1.23) may be written as

$$\dot{\hat{\rho}}_{\alpha\beta} = -\gamma\Phi^2\left(|\hat{\rho}_{\alpha\beta}|^2 - 1\right)\hat{\rho}_{\alpha\beta} + n_p\omega\mathcal{J}\rho_{\alpha\beta}, \tag{1.26}$$

while the estimation error $\tilde{\rho}_{\alpha\beta}$ satisfies

$$\dot{\tilde{\rho}}_{\alpha\beta} = -\gamma\Phi^2\left(|\tilde{\rho}_{\alpha\beta}|^2 + 2\tilde{\rho}_{\alpha\beta}^\top\rho_{\alpha\beta}\right)\left(\tilde{\rho}_{\alpha\beta} + \rho_{\alpha\beta}\right). \tag{1.27}$$

Proof. First, notice that $\tilde{\lambda} = \Phi\tilde{\rho}_{\alpha\beta}$, which replaced in (1.24) yields

$$\dot{\tilde{l}} = -\gamma\Phi^3\left(|\tilde{\rho}_{\alpha\beta}|^2 + 2\tilde{\rho}_{\alpha\beta}^\top\rho_{\alpha\beta}\right)\left(\tilde{\rho}_{\alpha\beta} + \rho_{\alpha\beta}\right)$$

leading directly to (1.27). Now, notice that $|\tilde{\rho}_{\alpha\beta}|^2 + 2\tilde{\rho}_{\alpha\beta}^\top\rho_{\alpha\beta} = |\hat{\rho}_{\alpha\beta}|^2 - 1$, while $\dot{\tilde{\rho}}_{\alpha\beta} = \dot{\hat{\rho}}_{\alpha\beta} - n_p\omega\mathcal{J}\rho_{\alpha\beta}$, which replaced in (1.27) yields (1.26). $\nabla\nabla\nabla$

1.7 An I&I speed and load torque observer

In this section an observer for the unmeasurable variables ω and τ_L is designed following the I&I methodology (Astolfi *et al.* 2007). The construction proceeds along the following steps.

S1. The parametrization of the mechanical dynamics—in terms of $\rho_{\alpha\beta}$—given in (1.3), as well as the representation of the flux observer (1.23) given in (1.26), are used.

[3] Notice the presence of the free adaptation gain γ on the lower bound.

S2. The term $\rho_{\alpha\beta}$ in both equations is decomposed as the sum of its estimate $\hat{\rho}_{\alpha\beta}$ and the error $\tilde{\rho}_{\alpha\beta}$, and we treat the latter as a perturbation.

S3. A globally exponentially convergent I&I observer of ω and τ_L is designed neglecting the perturbation in the system[4].

The mechanical equation (1.3) and the position observer (1.26) can be written in the "perturbed" form

$$\begin{aligned} J\dot{\omega} &= n_p\Phi i_{\alpha\beta}^\top \mathcal{J}\hat{\rho}_{\alpha\beta} - \tau_L - (n_p\Phi i_{\alpha\beta}^\top \mathcal{J}\tilde{\rho}_{\alpha\beta}) \\ \dot{\hat{\rho}}_{\alpha\beta} &= -\gamma\Phi^2\left(|\hat{\rho}_{\alpha\beta}|^2 - 1\right)\hat{\rho}_{\alpha\beta} + n_p\omega\mathcal{J}\hat{\rho}_{\alpha\beta} - (n_p\omega\mathcal{J}\tilde{\rho}_{\alpha\beta}). \end{aligned} \tag{1.28}$$

Their corresponding unperturbed forms, *i.e.*, with $\tilde{\rho}_{\alpha\beta} = 0$, are given by

$$\begin{aligned} J\dot{\omega} &= n_p\Phi i_{\alpha\beta}^\top \mathcal{J}\hat{\rho}_{\alpha\beta} - \tau_L \\ \dot{\hat{\rho}}_{\alpha\beta} &= -\gamma\Phi^2\left(|\hat{\rho}_{\alpha\beta}|^2 - 1\right)\hat{\rho}_{\alpha\beta} + n_p\omega\mathcal{J}\hat{\rho}_{\alpha\beta} \\ \dot{\tau}_L &= 0, \end{aligned} \tag{1.29}$$

where, for completeness, the last (trivial) equation has been added.

Proposition 1.7.1 *Consider the system (1.29) and the speed and load torque observer*

$$\begin{aligned} \dot{\xi} &= A_{33}\xi + \begin{bmatrix} \frac{a_2}{J} - n_p a_1^2 \\ n_p a_1 a_2 \end{bmatrix}\mathcal{A}\left(\frac{\hat{\rho}_\beta}{\hat{\rho}_\alpha}\right) + \begin{bmatrix} \frac{n_p\Phi}{J} i_{\alpha\beta}^\top \mathcal{J}\hat{\rho}_{\alpha\beta} \\ 0 \end{bmatrix} \\ \begin{bmatrix} \hat{\omega} \\ \hat{\tau}_L \end{bmatrix} &= \xi + \begin{bmatrix} a_1 \\ -a_2 \end{bmatrix}\mathcal{A}\left(\frac{\hat{\rho}_\beta}{\hat{\rho}_\alpha}\right) \end{aligned} \tag{1.30}$$

where $\mathcal{A}(\cdot)$ is an operator defined in Appendix A[5], and A_{33} is the Hurwitz matrix

$$A_{33} := \begin{bmatrix} -n_p a_1 & -\frac{1}{J} \\ n_p a_2 & 0 \end{bmatrix}, \quad a_1, a_2 > 0. \tag{1.31}$$

For some $\alpha > 0$ and for all initial conditions $(\omega(0), \xi(0)) \in \mathbf{R} \times \mathbf{R}^2$,

$$\lim_{t\to\infty} e^{\alpha t}\left|\begin{bmatrix} \hat{\omega}(t) - \omega(t) \\ \hat{\tau}_L(t) - \tau_L \end{bmatrix}\right| = 0. \tag{1.32}$$

That is, (1.30) is a globally exponentially convergent speed and load torque observer for the unperturbed system (1.29).

Proof. Following the I&I procedure (Astolfi *et al.* 2007), we define a manifold (in the extended state-space of the plant and the observer) that should be rendered attractive and invariant. As is well–known, to achieve the latter objective a partial differential equation (PDE) should be solved.

[4]The perturbation term that is neglected in this section is lumped into the overall error dynamics, whose stability is analyzed in Section 1.8.

[5]As explained below, the operator $\mathcal{A}(z)$, which is widely used in the drives community, is "essentially" equal to $\arctan(z)$, and is introduced to avoid singularities and jumps.

For the system (1.29) we propose the manifold

$$\mathcal{M} := \{(\xi, \omega, \hat{\rho}_{\alpha\beta}) : \xi - \begin{bmatrix} \omega \\ \tau_L \end{bmatrix} + \zeta(\hat{\rho}_{\alpha\beta}) = 0\} \subset \mathbf{R}^5, \tag{1.33}$$

where $\xi \in \mathbf{R}^2$ is the observer state, the dynamics of which are defined below, and the mapping $\zeta(\hat{\rho}_{\alpha\beta})$ is also to be defined.

To prove that the manifold $\mathcal{M}$ is attractive and invariant it is shown that the off–the–manifold coordinate

$$\chi_{67} := \xi - \begin{bmatrix} \omega \\ \tau_L \end{bmatrix} + \zeta(\hat{\rho}_{\alpha\beta}), \tag{1.34}$$

the norm of which determines the distance of the state to the manifold $\mathcal{M}$, is such that:

- $\chi_{67}(0) = 0 \Rightarrow \chi_{67}(t) = 0$, for all $t \geq 0$ (invariance);
- $\chi_{67}(t)$ asymptotically (*exponentially*) converges to zero (attractivity).

Notice that, if $\chi_{67}(t) \to 0$, an asymptotic estimate of $\begin{bmatrix} \omega \\ \tau_L \end{bmatrix}$ is given by $\xi + \zeta(\hat{\rho}_{\alpha\beta})$.

To obtain the dynamics of χ_{67} differentiate (1.34) along the trajectories of (1.29), yielding

$$\dot{\chi}_{67} = \dot{\xi} - \nabla\zeta[\gamma\Phi^2\left(|\hat{\rho}_{\alpha\beta}|^2 - 1\right)\hat{\rho}_{\alpha\beta} - n_p\omega\mathcal{J}\hat{\rho}_{\alpha\beta}] + \begin{bmatrix} \frac{\tau_L}{J} - \frac{n_p\Phi}{J} i_{\alpha\beta}^\top \mathcal{J}\hat{\rho}_{\alpha\beta} \\ 0 \end{bmatrix}$$

Our objective is to find $\dot{\xi}$ and a mapping ζ to obtain an asymptotically stable linear dynamics for χ_{67}. Towards this end, notice that selecting $\dot{\xi}$ as

$$\dot{\xi} = A_{33}(\xi + \zeta) + \gamma\Phi^2\left(|\hat{\rho}_{\alpha\beta}|^2 - 1\right)\nabla\zeta\hat{\rho}_{\alpha\beta} + \begin{bmatrix} \frac{n_p\Phi}{J} i_{\alpha\beta}^\top \mathcal{J}\hat{\rho}_{\alpha\beta} \\ 0 \end{bmatrix} \tag{1.35}$$

yields

$$\dot{\chi}_{67} = A_{33}(\xi + \zeta) + \begin{bmatrix} \frac{\tau_L}{J} \\ 0 \end{bmatrix} + n_p\omega\nabla\zeta\mathcal{J}\hat{\rho}_{\alpha\beta}.$$

Consequently, if we can solve the PDE

$$\nabla\zeta\mathcal{J}\hat{\rho}_{\alpha\beta} = \begin{bmatrix} a_1 \\ -a_2 \end{bmatrix}, \tag{1.36}$$

recalling (1.34), one gets

$$\dot{\chi}_{67} = A_{33}\chi_{67}, \tag{1.37}$$

as desired. The PDE (1.36), indeed, has a solution

$$\zeta(\hat{\rho}_{\alpha\beta}) = \begin{bmatrix} a_1 \\ -a_2 \end{bmatrix} \arctan\left(\frac{\hat{\rho}_\beta}{\hat{\rho}_\alpha}\right). \tag{1.38}$$

Now, with the definition above,

$$\nabla\zeta = \frac{-1}{|\hat{\rho}_{\alpha\beta}|^2} \begin{bmatrix} a_1 \\ -a_2 \end{bmatrix} \hat{\rho}_{\alpha\beta}^\top \mathcal{J}.$$

Consequently $\nabla\zeta\hat{\rho}_{\alpha\beta} = 0$, and the second right hand term in (1.35) vanishes. The proof is completed noting that

$$A_{33}\begin{bmatrix} a_1 \\ -a_2 \end{bmatrix} = \begin{bmatrix} \frac{a_2}{J} - n_p a_1^2 \\ n_p a_1 a_2 \end{bmatrix},$$

replacing the function $\arctan$ by the operator $\mathcal{A}$ in (1.30), and noting that the derivations above remain valid after this substitution. $\nabla\nabla\nabla$

Remark 5. If the $\arctan$ function is used instead of the operator $\mathcal{A}$ in order to recover the estimate $\hat{\rho}_{\alpha\beta}$, some Dirac delta functions might appear in the speed estimation and the error dynamics. To explain this phenomenon consider the case of (constant) regulation of the motor speed and assume that $\hat{\rho}_{\alpha\beta}(t) \equiv \rho_{\alpha\beta}(t)$. Then, in view of (1.38), we have that $\zeta(\hat{\rho}_{\alpha\beta}(t)) \equiv \theta(t) = \omega^\star t (\mathtt{mod}\ \pi)$, which is a periodic function defined on the set $(-\pi, \pi)$. In this scenario the $\arctan$ jumps instantaneously from the value $\frac{\pi}{2}$ to the value $\frac{-\pi}{2}$ inducing a train of Dirac delta functions, $\delta_T(t)$, in the derivative of $\arctan$. This term propagates, through $\dot{\zeta}(\rho_{\alpha\beta})$, into the error dynamics that now reads as[6]

$$\dot{\chi}_{67} = \begin{bmatrix} -n_p a_1 & -\frac{1}{J} \\ n_p a_2 & 0 \end{bmatrix}\chi_{67} + \begin{bmatrix} a_1 \\ -a_2 \end{bmatrix}\delta_T.$$

As illustrated in the simulations of Section 1.9 this undesirable effect is removed using instead the operator $\mathcal{A}$ defined in Appendix A.

Remark 6. Proposition 1.7.1 refers to the unperturbed dynamics (1.29), for which it was assumed that $\tilde{\rho}_{\alpha\beta} = 0$. Some simple calculations show that if this term is not zero the error dynamic of χ_{67} takes the form

$$\dot{\chi}_{67} = \begin{bmatrix} -n_p a_1 & -\frac{1}{J} \\ n_p a_2 & 0 \end{bmatrix}\chi_{67} - \frac{n_p\omega}{|\hat{\rho}_{\alpha\beta}|^2}\begin{bmatrix} a_1 \\ -a_2 \end{bmatrix}\hat{\rho}_{\alpha\beta}^\top\tilde{\rho}_{\alpha\beta} + \begin{bmatrix} \frac{n_p\Phi}{J} i_{\alpha\beta}^\top \mathcal{J}\tilde{\rho}_{\alpha\beta} \\ 0 \end{bmatrix} \tag{1.39}$$

In the next section the effect of the additional terms on the overall dynamics is analyzed.

1.8 Proof of the main result

In this section the stability properties of the closed–loop system, composed by the motor (1.7), the output–feedback controller (1.18), the position observer (1.23), (1.25) and the speed–load torque observer (1.30) are studied.

The dynamics are described using the error coordinates (1.9), which yields a set of nonlinear differential equations of the form (1.10). For ease of reference, these equations are sequentially derived for χ_{13}, χ_{45} and χ_{67}. The stability properties of the system are established invoking Lyapunov's indirect method. Towards this end, the equations are written in the form

$$\dot{\chi} = A\chi + \Gamma(\chi), \tag{1.40}$$

where A is the system matrix of the linearized system, i.e. $A := \nabla f(0)$, where $f(\chi)$ is defined in (1.9), (1.10), and the elements of the vector $\Gamma(\chi)$ contain (second or higher order) products of the components of χ. The proof of the claim of asymptotic stability of Proposition 1.3.1, follows showing that A is a Hurwitz matrix.

[6]The expression above shows that, away from the isolated points where the δ–functions appear, the observer error exponentially converges to zero.

1.8.1 Currents and speed tracking errors

Lemma 1.8.1 *Consider the PMSM model (1.7) in closed–loop with the output–feedback controller (1.18). The first three components, χ_{13}, of the error vector χ—defined in (1.9)—evolve according to the following dynamics*

$$\dot{\chi}_{13} = A_{11}\chi_{13} + A_{12}\chi_{45} + A_{13}\chi_{67} + \Gamma_{13}(\chi) \tag{1.41}$$

where

$$\begin{aligned}
A_{11} &= F_d(x^*)Q \\
A_{12} &= \begin{bmatrix} -\frac{L}{J\Phi}\tau_L x_3^* & -dx_2^* - \frac{n_p\Phi}{J}x_3^* - \frac{r}{n_p\Phi}\tau_L \\ dx_2^* + \frac{n_p\Phi}{J}x_3^* + \frac{r}{n_p\Phi}\tau_L & -\frac{L}{J\Phi}\tau_L x_3^* \\ 0 & 0 \end{bmatrix} \\
A_{13} &= \begin{bmatrix} -\frac{L}{\Phi}\tau_L & -\frac{L}{J\Phi}x_3^* \\ 0 & \frac{r}{n_p\Phi} \\ 0 & 0 \end{bmatrix}
\end{aligned} \tag{1.42}$$

where $d = \frac{R-r}{L}$ while $F_d(x)$ and Q are defined in (1.17) and (1.12), respectively, and $\Gamma_{13}(\chi)$ is such that $\nabla\Gamma_{13}(0) = 0$. Moreover, the matrix A_{11} is Hurwitz.

Proof. The output–feedback controller (1.18) can be written as

$$v_{\alpha\beta} = [\tilde{\rho}_\alpha I_2 + \tilde{\rho}_\beta \mathcal{J}]\,\hat{v} + e^{\mathcal{J}\theta}\hat{v},$$

which, in dq coordinates, *i.e.*, considering $v = e^{-\mathcal{J}\theta}v_{\alpha\beta}$, takes the form

$$v = \hat{v} + [\hat{v}_1 I_2 + \hat{v}_2\mathcal{J}]\,\chi_{45} \tag{1.43}$$

where we have used the errors $\chi_{45} = e^{-\mathcal{J}\theta}\tilde{\rho}_{\alpha\beta}$, and $\hat{v}_1$ and $\hat{v}_2$ are the components of $\hat{v}$.

On the other hand, some simple calculations show that

$$\hat{v} = v^{FI} + \begin{bmatrix} -\frac{L}{\Phi}\tau_L & -\frac{L}{J\Phi}x_3^* \\ 0 & \frac{r}{n_p\Phi} \end{bmatrix}\chi_{67} - \begin{bmatrix} \frac{L\chi_7}{\Phi}(\frac{1}{J}\chi_3 + \chi_6) \\ 0 \end{bmatrix}$$

with the full–information control v^{FI} given by (1.16). Using the definition of χ_3, the latter can be decomposed as

$$v^{FI} = dx_{12} + \begin{bmatrix} -\frac{L}{J\Phi}\tau_L x_3^* \\ \frac{n_p\Phi}{J}x_3^* + \frac{r}{n_p\Phi}\tau_L \end{bmatrix} + \begin{bmatrix} -\frac{L}{J\Phi}\tau_L\chi_3 \\ 0 \end{bmatrix}.$$

Finally, the second term of the control law v can be expanded as

$$[\hat{v}_1 I_2 + \hat{v}_2\mathcal{J}]\,\chi_{45} = \begin{bmatrix} -\frac{L}{J\Phi}\tau_L x_3^* & -dx_2^* - \frac{n_p\Phi}{J}x_3^* - \frac{r}{n_p\Phi}\tau_L \\ dx_2^* + \frac{n_p\Phi}{J}x_3^* + \frac{r}{n_p\Phi}\tau_L & -\frac{L}{J\Phi}\tau_L x_3^* \end{bmatrix}\chi_{45} + \Gamma_{13}(\chi)$$

for some $\Gamma_{13}(\chi)$ verifying the conditions of the lemma. Using all the expressions above to define v, and replacing in (1.13), yields (1.41), (1.42) allowing to complete the first part of the proof.

To prove that the matrix A_{11} is Hurwitz we use (1.17) and (1.12) to evaluate

$$F_d(x^*)Q = \begin{bmatrix} -\frac{r}{L} & \frac{n_p}{J}x_3^* & 0 \\ -\frac{n_p}{J}x_3^* & -\frac{r}{L} & -\frac{n_p\Phi}{J} \\ 0 & \frac{n_p\Phi}{L} & 0 \end{bmatrix}.$$

Some simple calculations show that the characteristic polynomial is of the form $s^3 + c_1 s^2 + c_2 s + c_3$, with the coefficients $c_i > 0$ and verifying $c_1 c_2 > c_3$ that, a simple Routh–Hurwitz test, proves is the necessary and sufficient condition for stability. $\nabla\nabla\nabla$

1.8.2 Estimation error for $\rho_{\alpha\beta}$

Lemma 1.8.2 *Consider the mechanical equation of the PMSM model (1.4) together with the flux observer (1.23). The fourth and fifth components, χ_{45}, of the error vector χ—defined in (1.9)—satisfy the following differential equation*

$$\dot{\chi}_{45} = A_{22}\chi_{45} + \Gamma_{45}(\chi) \tag{1.44}$$

with

$$A_{22} = \begin{bmatrix} -2\gamma\Phi^2 & \frac{n_p}{J}x_3^\star \\ -\frac{n_p}{J}x_3^\star & 0 \end{bmatrix} \tag{1.45}$$

and $\Gamma_{45}(\chi)$ is such that $\nabla\Gamma_{45}(0) = 0$. Moreover, the matrix A_{22} is Hurwitz for all $x_3^\star \neq 0$.

Proof. Computing the time derivative of $\chi_{45} = e^{-\mathcal{J}\theta}\tilde{\rho}_{\alpha\beta}$ yields

$$\dot{\chi}_{45} = -\frac{n_p}{J}x_3\mathcal{J}\chi_{45} + e^{-\mathcal{J}\theta}\dot{\tilde{\rho}}_{\alpha\beta}.$$

Now, from (1.27), and using the facts that $|\tilde{\rho}_{\alpha\beta}| = |\chi_{45}|$ and that $e^{-\mathcal{J}\theta}\rho_{\alpha\beta} = e_1$, it is possible to write

$$\dot{\tilde{\rho}}_{\alpha\beta} = -\gamma\Phi^2\left(|\chi_{45}|^2 + 2\chi_{45}^\top e_1\right)e^{\mathcal{J}\theta}\left(\chi_{45} + e_1\right)$$

Replacing the latter in the expression above yields

$$\dot{\chi}_{45} = -\left[\frac{n_p}{J}(x_3^\star + \chi_3)\mathcal{J} + \gamma\Phi^2\left(|\chi_{45}|^2 + 2\chi_4\right)\right]\chi_{45} - \gamma\Phi^2\left(|\chi_{45}|^2 + 2\chi_4\right)e_1,$$

which concludes the first part of the proof.

The proof that, for all $x_3^\star \neq 0$, A_{22} is Hurwitz follows trivially computing the characteristic polynomial.

$\nabla\nabla\nabla$

1.8.3 Speed and load torque estimation errors

Lemma 1.8.3 *Consider the mechanical equations of the PMSM model (1.3), (1.4) together with the flux observer (1.23). The sixth and seventh components, χ_{67}, of the error vector χ—defined in (1.9)—satisfy the following differential equation*

$$\dot{\chi}_{67} = A_{32}\chi_{45} + A_{33}\chi_{67} + \Gamma_{67}(\chi), \tag{1.46}$$

where

$$A_{32} = \begin{bmatrix} -\frac{n_p}{J}\left(a_1 x_3^\star - \frac{\Phi x_2^\star}{L}\right) & 0 \\ \frac{n_p}{J} a_2 x_3^\star & 0 \end{bmatrix}, \tag{1.47}$$

A_{33} the Hurwitz matrix defined in (1.31), and $\Gamma_{67}(\chi)$ is such that $\nabla\Gamma_{67}(0) = 0$.

Proof. As indicated in Remark 6, the dynamics of χ_{67} is given by (1.39). For the last right–hand term we have the identity

$$i_{\alpha\beta}^\top \mathcal{J}\tilde{\rho}_{\alpha\beta} = \frac{1}{L}\chi_{12}^\top \mathcal{J}\chi_{45} + \frac{1}{L}(x_{12}^\star)^\top \mathcal{J}\chi_{45} \tag{1.48}$$

where x_{12}, defined in (1.11), is the stator current in the dq reference frame. On the other hand, after some lengthy but straightforward computations, the second right–hand term of (1.39) can be written as

$$\frac{n_p\omega}{|\hat{\rho}_{\alpha\beta}|^2}\hat{\rho}_{\alpha\beta}^\top\tilde{\rho}_{\alpha\beta} = \frac{n_p}{J}\left(x_3^\star + \chi_3\right)\chi_4 + \Omega(|\chi|^2), \tag{1.49}$$

where $\Omega(|\chi|^2)$ contains term of order higher or equal to $|\chi|^2$. Thus, the proof follows immediately by considering that $x_1^\star = 0$ and replacing (1.48) and (1.49) in (1.39). $\nabla\nabla\nabla$

1.8.4 Proof of Proposition 1.3.1

Combining the results of Lemmata 1–3 we obtain that the error vector χ satisfies a differential equation of the form (1.40) where

$$A = \begin{bmatrix} A_{11} & A_{12} & A_{13} \\ 0 & A_{22} & 0 \\ 0 & A_{32} & A_{33} \end{bmatrix}, \quad \Gamma(\chi) = \begin{bmatrix} \Gamma_{13}(\chi) \\ \Gamma_{45}(\chi) \\ \Gamma_{67}(\chi) \end{bmatrix}.$$

Recalling that $\nabla\Gamma(0) = 0$, it only remains to prove that A is Hurwitz. For, we notice that A is similar to a block triangular Hurwitz matrix. More precisely, with

$$T = \begin{bmatrix} I_3 & 0 & 0 \\ 0 & 0 & I_2 \\ 0 & I_2 & 0 \end{bmatrix},$$

we get

$$TAT^{-1} = \begin{bmatrix} A_{11} & A_{12} & A_{13} \\ 0 & A_{33} & A_{32} \\ 0 & 0 & A_{22} \end{bmatrix},$$

which is Hurwitz due to the fact that A_{11}, A_{22} and A_{33} are Hurwitz matrices, completing the proof. $\nabla\nabla\nabla$

1.9 Simulation and experimental results

The usefulness of the proposed control scheme was evaluated through numerical simulations and experiments. For the simulations, the considered motor parameters were $L = 0.0038H$, $R = 0.225\Omega$, $\Phi = 0.17Wb$, $n_p = 3$ and $J = 0.012kg.m^2$, which correspond to an experimental setup located in the *Laboratoire de Genie Electrique de Paris*, where the experiments were carried out.

1.9.1 Simulation results

Three types of simulations were developed, the first was devoted to illustrate the performance under nominal (ideal) conditions, where the motor parameters are known, while the second was intended to exhibit the operation under several cases of parametric uncertainty. Finally, we carried out a third set of simulations to compare the performance of the proposed scheme with one proposed in the drives community, namely the one reported in Nam (2010). The signal profiles and the parameter variations were taken from the benchmark proposed by the French Working Group *Commande des Entraînements Electriques*[7].

In order to evaluate the scheme under stringent conditions, the motor was at standstill at the beginning of the simulations. Hence, the initial conditions for both currents and speed, as well as, the initial values for the estimated speed and load torque were set to zero. To avoid singularities, the initial conditions of the position observer were set as $\hat{\rho}_\alpha(0) = \Phi$ and $\hat{\rho}_\beta(0) = 0$. On the other hand, from $t = 1s$ to $t = 2.5s$ and from $t = 5s$ to the end of the experiment, a $1Nm$ load torque was applied.

The tuning parameters of the control scheme were chosen as $\gamma = 5000$, for the $\rho_{\alpha\beta}$ observer, and $a_1 = 20$, $a_2 = 6$, for the speed–load torque observer. In both cases the selection was taken to obtain a better response of the closed–loop system under parametric uncertainty operation. The high value assigned to the gain γ is due to the high sensitivity exhibited by the position observer with respect to the stator resistance R.

In Figure 1.1 the behavior of the motor speed and the load torque are included under nominal operation. In the top of this figure, both the actual and the desired speeds are shown. Here it can be noticed that, as predicted by the theory, when the desired speed is constant the achieved performance is remarkable. Moreover, when the speed reference is time–varying the speed error still remains within reasonable values. In the bottom of the same figure the actual load torque and its estimate are presented. In Figure 1.2 the corresponding observation errors for the position and the speed–load toque observers are presented. In both cases their magnitudes are negligible, even in the presence of changes in the load torque perturbation and under time–varying speed references. This picture is complemented with the tracking speed error. In Figure 1.3 the stator currents and voltages are presented.

To illustrate the controller robustness against parametric uncertainty, in Figure 1.4 the observer and speed tracking errors corresponding to a 50% positive variation of the stator resistance value are depicted, while the behavior of the same variables for a 50% increase of the stator inductance and a 15% positive change of the field flux are included in Figure 1.5 and Figure 1.6, respectively. It is important to mention that these parameter variations correspond to the maximum uncertainty that the controller can manage without going to instability.

In Nam (2010), see also Lee *et al.* (2010), the observer of Ortega *et al.* (2011) is used together with a phase–locked–loop like speed and load torque observer to implement an output feedback version of the classical field–oriented controller Krause (1986). To compare the performance of our new speed and load torque observer and the proposed IDA–PBC, we show in Figure 1.7 the response of both schemes to the previous benchmark references. It is clear from the figure that our scheme outperforms the one in Nam (2010), both in speed regulation as well as load torque estimation.

[7]The complete evaluation procedure can be consulted in `http://www2.irccyn.ec-nantes.fr/CE2/`.

1.9.2 Experimental results

Experiments were carried out to test the performance of the proposed controller. Unfortunately, at the moment of writing this paper the evaluation of the *full–information* IDA–PBC and the observers was carried out in a separated way, *i.e.*, it was not possible to present the output–feedback operation. The behavior of the several components is depicted in Figure 1.8 for a positive speed reference, while in Figures 1.9 and 1.10 the operation for a speed reference that crosses through zero is shown.

1.10 Future research

From a theoretical viewpoint the need to include the operator $\mathcal{A}\left(\frac{\hat{\rho}_\beta}{\hat{\rho}_\alpha}\right)$ to avoid the presence of spikes may seem unsatisfactory. However, in practice this kind of modifications are systematically applied and widely accepted. Given the theoretical complexity of the problem we tend to believe that the problem does not admit a "smooth" solution. The result is presented without a detailed analysis of the effect of this operator—that is currently under investigation.

Another research line that we are currently pursuing is the establishment of a non–conservative estimate of the region of attraction of the equilibrium point. It has been observed in simulations that the estimates that are obtained with the standard Lyapunov tools are extremely conservative and provide little insight on the choice of the free parameters γ, a_1 and a_2. This research is, obviously, related with the analysis of the full–fledged nonlinear dynamics, that seems a formidable task.

Simulations have shown that performance is sensitive to parameter uncertainty, in particular in the field flux. To enhance robustness it would be interesting to incorporate an adaptation algorithm, but this task is far from trivial given the nonlinearly parameterized nature of the problem. Robustness can also be enhanced trying alternative solutions for the PDE's that appear in the IDA–PBC and the I&I design methodologies.

Some preliminary experimental results, which have confirmed the remarkable properties of the observers, have been reported here. Current research is under way to try experimentally the output–feedback controller proposed in the paper.

Acknowledgments. Part of the work of Gerardo Espinosa–Pérez was developed during a sabbatical leave at LSS–SUPELEC supported by SUPELEC Foundation. Currently his work is supported by DGAPA–UNAM (IN111211). The work of Dhruv Shah was supported by the Indo–French project No. 3602-1, under the aegis of IFCPAR. The authors want to thanks to Alain Glumineau and Robert Boisliveau (IRCCyN, France) for the computational code to generate the operator $\mathcal{A}$.

References

Akrad A, Hilairet M., Ortega R and Diallo D 2007 Interconnection and damping assignment approach for reliable pm synchronous motor control. *Colloquium On Reliability in Electromagnetic Systems*, Paris, France.

Astolfi A, Karagiannis D and Ortega R 2007 *Nonlinear and Adaptive Control with Applications*. Springer-Verlag, Berlin, Communications and Control Engineering.

Chiasson J 2005 *Modeling and High Performance Control of Electric Machines*, Wiley.

Dawson D, Hu J and Burg T, *Nonlinear Control of Electric Machinery*, Marcel Dekker.

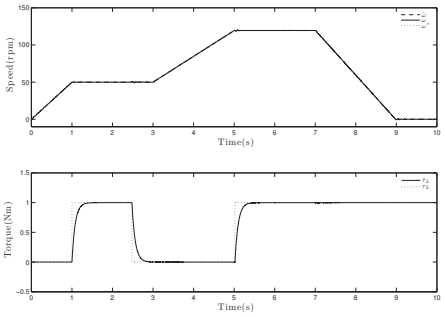

Figure 1.1 *Reference and actual speed (top) and load torque and its estimate (bottom) in nominal operation*

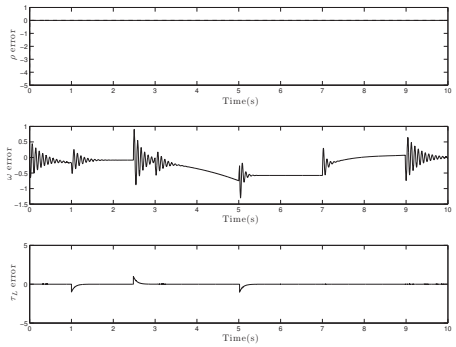

Figure 1.2 *Observer and speed tracking errors in nominal operation*

Ezzat M, de Leon J, Gonzalez N and Glumineau A 2010 Observer–controller scheme using high order sliding mode techniques for sensorless speed control of permanent magnet synchronous motor. *49th IEEE Conference on Decision and Control*, Atlanta, Georgia, USA.

Ezzat M, Glumineau A and Plestan F 2010 Sensorless speed control of a permanent magnet synchronous motor: high order sliding mode controller and sliding mode control observer. *8th IFAC Symposium on Nonlinear Control Systems*, Bologne, Italy.

Fabio G, Miceli R, Rando C and Ricco–Galluzzo G 2010 Back EMF sensorless-control algorithm for high-dynamic performance PMSM. *IEEE Transactions on Industrial Electronics* **57–6**, 2092–2100.

Ichikawa S, Tomita M, Doki S and Okuma S 2006 Sensorless control of PMSM using on-line parameter identification based on system's identification theory. *IEEE Trans Industrial Electronics* **53–2**, 363–373.

Khorrami F, Krishnamurthy P and Melkote H 2003 *Modeling and Adaptive Nonlinear Control of Electric Motors*, Springer, Heidelberg.

Krause PC 1986 *Analysis of Electric Machinery*, McGraw Hill, New York.

Lee J, Hong J, Nam K, Ortega R, Astolfi A and Praly L 2010 Sensorless control of surface-mount permanent magnet synchronous motors based on a nonlinear observer. *IEEE Transactions on Power Electronics* **25–2**, 290–297.

Marino R, Tomei P and Verrelli CM 2008 Adaptive field-oriented control of synchronous motors with damping windings. *European Journal of Control* **14–3**, 177–196.

Matsui N 1996 Sensorless PM brushless DC motor drives. *IEEE Trans Industrial Electronics*, **43–2**, 300–308.

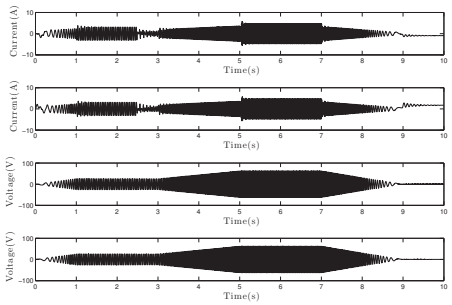

Figure 1.3 *Stator currents and voltages in nominal operation*

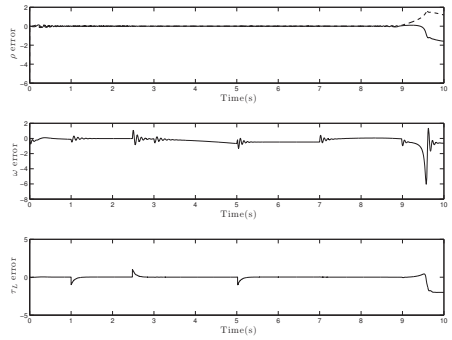

Figure 1.4 *Observer and speed tracking errors with a* 50% *error of the stator resistance*

Montanari M, Peresada S and Tilli A 2006 A speed sensorless indirect field oriented control for induction motors based on high–gain speed estimation. *Automatica* **42**, 1637–1650.

Nahid Mobarakeh B, Meibody–Tabar F and Sargos F 2001 Robustness study of a model–based technique for mechanical sensorless control of PMSM. *Power Electronics Specialist Conference (PESC'2001)*, Vancouver, Canada.

Nam K 2010 *AC Motor Control and Electric Vehicle Applications*, CRC Press.

Ortega R, van der Schaft AJ, Maschke BM and Escobar G 2002 Interconnection and damping assignment passivity-based control of port-controlled Hamiltonian systems. *Automatica* **38–4**, 585-596.

Ortega R and Garcia-Canseco E 2004 Interconnection and damping assignment passivity-based control: A survey. *European Journal of Control* **10**, 432–450.

Ortega R, Loria A, Nicklasson PJ and Sira-Ramírez H 1998 *Passivity–based Control of Euler–Lagrange Systems*, Springer-verlag, Berlin, Communications and Control Engineering.

Ortega R, Praly L, Astolfi A, Lee J and Nam K 2011 Estimation of rotor position and speed of permanent magnet synchronous motors with guaranteed stability. *IEEE Transaction on Control Systems Technology* **19–2**, 284–296.

Petrovic V, Ortega R and Stankovic A 2001 Interconnection and damping assignment approach to control of PM synchronous motor. *IEEE Trans. Control Syst. Techn* **9–6**, 811–820.

Rajashekara K, Kawamura A and Matsuse K 1996 *Sensorless Control of AC Motor Drives*, IEEE Press.

Shah D, Ortega R and Astolfi A 2009 Speed and load torque observer for rotating machines. *48th IEEE Conference on Decision and Control*, Shangai, China.

Tomei P and Verrelli CM A nonlinear adaptive speed tracking control for sensorless permanent magnet step motors with unknown load torque. *International Journal of Adaptive Control and Signal Processing* **22–3**, 266–288.

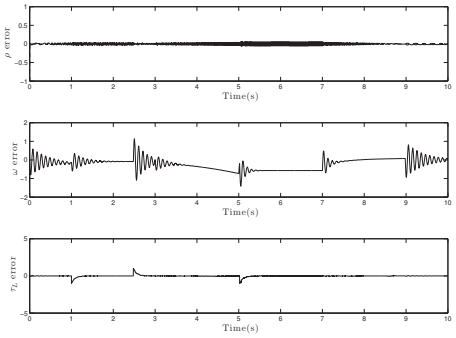

Figure 1.5 *Observer and speed tracking errors with a* 50% *increase of the stator inductance*

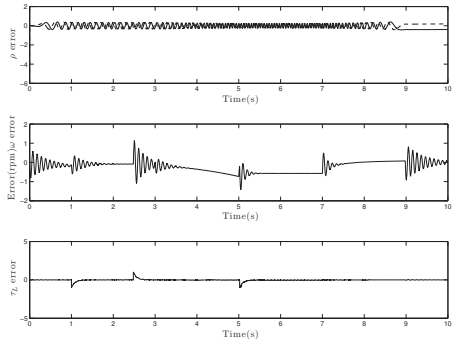

Figure 1.6 *Observer and speed tracking errors with a* 15% *positive increase of the field flux*

van der Schaft AJ 2000 $\mathcal{L}_2$*-Gain and passivity techniques in nonlinear control*, Springer-verlag, Berlin.
Zaltni D, Naceur M, Ghanes M and Barbot JP 2008 Observability analysis of PMSM. *2009 International Conference on Signals, Circuits and Systems*, Jerba, Tunisia.

Appendix A

In computer programming languages the single argument $\arctan(u)$ function is computed in such a way that its output value e is wrapped in the set $(-\pi, \pi]$. This situation results in the existence of discontinuities since each time the output of the function e takes a value higher (lower) than π (resp;,$-\pi$) then it is assigned the value $-\pi$ (resp.,π). With the aim of avoiding these discontinuities it is usual practice to modify the $arctan(u)$ function by including at its output an additional block whose input is e, the output of the $\arctan$ function, and its output is given by

$$y = e + 2n\pi$$

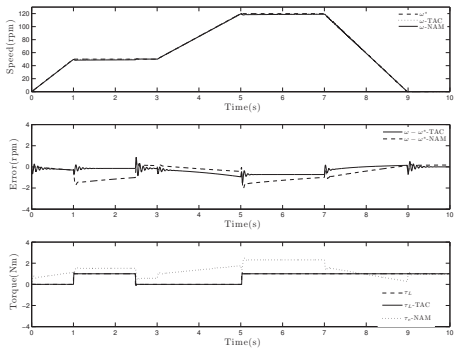

Figure 1.7 *Comparative behavior of the proposed scheme (denoted TAC) with the one reported in Nam (2010) (denoted NAM)*

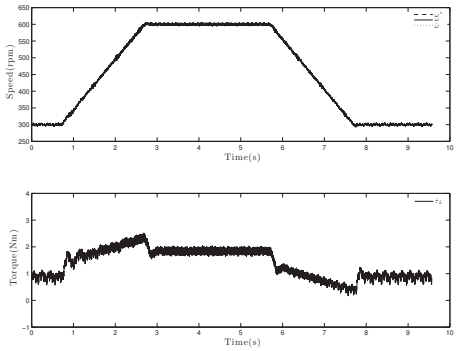

Figure 1.8 *Reference, measured and actual speeds (top) and observed load torque (bottom) in the experimental rig*

where n is a counter, initialized at zero, that is increased by 1 each time the $e > \pi$ or decreased by 1 if $e < -\pi$. From a mathematical perspective, the result is an operator, denoted as $\mathcal{A}(u)$, that has as input the argument of the $\arctan$ function and as output a continuous variable that corresponds to the unwrapped version of the original output of the $\arctan$ function.

It is clear that $\mathcal{A}(u)$ can be easily implemented in any programming language, like *C* or *Matlab*. The code for doing this considers two consecutive values of e at two consecutive sampling times, kT, $(k+1)T$, and compute its difference $dif = e[kT] - e[(k+1)T]$ in order to know if there has been a jump from π to $-\pi$ or viceversa. According to this, three different possibilities can appear:

- If $dif < -2\pi$ then $n = n + 1$.

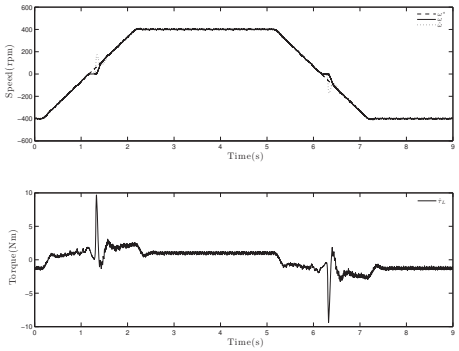

Figure 1.9 *Measured and observed speed (top) and estimated load torque (bottom) in the experimental rig*

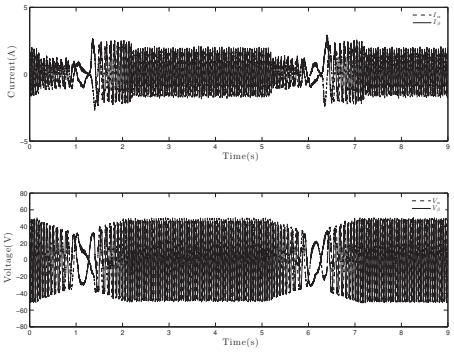

Figure 1.10 *Current (top) and voltage (bottom) in the experimental rig*

- If $dif > 2\pi$ then $n = n - 1$.
- Otherwise the value of n is not changed.

The computational loop is closed by updating the value of y and assigning $k = k + 1$.